Journal of Alloys and Compounds 509 (2011) 4010–4013

Contents lists available at ScienceDirect

Journal of Alloys and Compounds

journal homepage: www.elsevier.com/locate/jallcom

FeCoHfN thin films fabricated by co-sputtering with high resonance frequency

Nguyen Nguyen Phuoc[a,*], Le Thanh Hung[b], C.K. Ong[b]

[a] Temasek Laboratories, National University of Singapore, 5A Engineering Drive 2, Singapore 117411, Singapore
[b] Center for Superconducting and Magnetic Materials, Department of Physics, National University of Singapore, 2 Science Drive 3, Singapore 117542, Singapore

ARTICLE INFO

Article history:
Received 26 November 2010
Received in revised form
28 December 2010
Accepted 30 December 2010
Available online 4 January 2011

Keywords:
Soft magnetic thin films
Resonance frequency
Dynamic permeability
Rotatable anisotropy

ABSTRACT

Thin films of FeCoHfN were fabricated by co-sputtering technique with the deposition angles varied. Their dynamic magnetic properties were characterized and discussed in conjunction with an analysis based on Landau–Lifshitz–Gilbert equation. High ferromagnetic resonance frequency beyond 6 GHz was achieved by adjusting the deposition angle. A discrepancy between static and magnetic anisotropy was observed and discussed within the framework of Hoffmann's ripple theory. Also, the variations of frequency linewidth, damping factor, and permeability with the change of deposition angle were presented and discussed.

1. Introduction

Compared to conventional bulk magnetic materials, magnetic thin films possess a much higher dynamic permeability in gigahertz frequency range making them promising candidates for high frequency magnetic devices such as micro inductors and electromagnetic noise absorbing components [1–3]. When using magnetic materials designated for microwave applications, one of the most important parameters to be considered is the ferromagnetic resonance frequency [2,3]. At the frequency beyond the resonance frequency, permeability is close to unity which is of no use to most of the microwave applications [4]. In other words, the resonance frequency determines the operating frequency range for microwave devices. Nowadays, as the operating frequency in many devices reaches gigahertz, for instance the typical frequencies for Bluetooth technology are 2.4 and 5.8 GHz, the need for magnetic thin films with high resonance frequency is indispensable [2,3]. Among various materials, thin films based on FeCo alloy such as FeCoN [1], FeCoB [5–7], FeCo–SiO_2 [2,8], FeCo–Al_2O_3 [9], FeCo–SiN [10], FeCo–HfO [11] and FeCo–HfN [12,13] have received much attention due to their relatively high saturation magnetization. In this paper, we report the investigation of magnetic dynamic properties of FeCoHfN thin films grown by co-sputtering of FeCo and Hf. By changing substrate position so as the deposition angle is varied, we can tailor not only the resonance frequency but also the frequency linewidth to meet the demand for microwave application using magnetic thin films.

2. Experimental

A schematic picture of our co-sputtering deposition system is shown in Fig. 1. Two sputtering sources with $Fe_{70}Co_{30}$ and Hf targets were employed and Mylar substrates (50 μm thick) with the size of 5 mm × 10 mm were put on a substrate holder facing the FeCo target. The deposition angle β is defined as the off-center angle of FeCo target as illustrated in Fig. 1. A series of FeCoHfN thin films was fabricated at ambient temperature with various deposition angles β. Each sample in the series was deposited at one run and the thickness of the sample was fixed at 100 nm which was controlled by deposition time and verified by thickness profilemeter. The base pressure better than 7×10^{-7} Torr and the working pressure was kept at 10^{-3} Torr during the deposition process by introducing argon mixed with 3% nitrogen gas at the flow rate of 16 SCCM (SCCM denotes cubic centimeter per minute at STP). A magnetic field of about 200 Oe was applied in the plane of the films along the easy axis shown in Fig. 1. The composition of the samples was preliminarily determined by deposition rate of each target and was subsequently verified by Energy Dispersive X-ray Spectroscope (EDS). The variation of composition of each component in FeCoHfN thin films with deposition angle β is shown in Fig. 2. It is seen that the component of Hf is increased with the increase of deposition angle β and at the same time the contribution of FeCo is reduced. Although the plasma shape of our sputtering system is conical as illustrated in Fig. 1 the density of deposition rate is not uniform through out the whole area. In particular, the deposition rate at the center is higher than that off the center. As a result the deposition rate of FeCo is decreased with deposition angle β while the deposition rate of Hf is increased and this explains why the composition of FeCoHfN is varied as in Fig. 2. An M–H loop tracer was employed to measure the hysteresis loops of the samples at room temperature. The permeability spectra over the frequency range from 0.05 GHz to 8 GHz were obtained by a shorted micro-strip transmission-line perturbation method using a fixture developed in our laboratory. Further details of this method can be found in a previous paper [14].

* Corresponding author. Tel.: +65 65162816; fax: +65 67776126.
E-mail addresses: tslnnp@nus.edu.sg, nnguyenphuoc@yahoo.com (N.N. Phuoc).

0925-8388/$ – see front matter © 2011 Elsevier B.V. All rights reserved.
doi:10.1016/j.jallcom.2010.12.208

3. Results and discussion

The hysteresis loops measured along easy and hard axes at room temperature for two samples deposited at the deposition angle $\beta = 0^\circ$ and $\beta = 18^\circ$ are shown in Fig. 3(a) and (b). The sample grown at $\beta = 18^\circ$ clearly shows a more slanted hard axis curve than the sample grown at $\beta = 0^\circ$ indicating that the magnetic anisotropy field in sample at $\beta = 18^\circ$ is larger. This enhancement of uniaxial anisotropy field with the off-center of substrate position is similar to that observed in oblique deposition [5–7,15] and may be interpreted in the same way. It is generally accepted in the literature that the mechanism of the oblique incidence anisotropy is due to induced uniaxial stress anisotropy, a modification of the short range order and/or columnar growth morphology with increasing oblique angle [5,6]. As a result of the improvement of uniaxial anisotropy, the FMR frequency of the off-center sample is increased which manifests itself as the shift of the peak of the imaginary permeability curve to higher frequency range as in Fig. 3(c) and (d). For sample grown at $\beta = 0^\circ$, the FMR frequency is around 3.66 GHz while it is increased up to 6.43 GHz with the sample fabricated at $\beta = 18^\circ$. For a more quantitative examination, an analysis based on the Landau–Lifshitz–Gilbert (LLG) equation was employed.

As is well known, the dynamic magnetization behavior of the thin film can be described by the LLG equation [16]

$$\frac{d\vec{M}}{dt} = -\gamma(\vec{M} \times \vec{H}) + \frac{\alpha_{\text{eff}}}{M}\vec{M} \times \frac{d\vec{M}}{dt} \tag{1}$$

where M represents the magnetic moment, H is the magnetic field, α_{eff} is the dimensionless effective damping coefficient (α_{eff} is not intrinsic but takes into account all possible effects of damping) and γ is the gyromagnetic ratio. By solving the LLG equation, one can readily obtain the complex permeability as follows [8,16]:

$$\mu' = 1 + 4\pi M_{\text{eff}}\gamma^2 \frac{(4\pi M_{\text{eff}} + H_{\text{K}}^{\text{dyn}})(1+\alpha_{\text{eff}}^2)[\omega_{\text{R}}^2(1+\alpha_{\text{eff}}^2) - \omega^2] + (4\pi M_{\text{eff}} + 2H_{\text{K}}^{\text{dyn}})(\alpha_{\text{eff}}\omega)^2}{[\omega_{\text{R}}^2(1+\alpha_{\text{eff}}^2) - \omega^2]^2 + [\alpha_{\text{eff}}\omega\gamma(4\pi M_{\text{eff}} + 2H_{\text{K}}^{\text{dyn}})]^2} \tag{2}$$

$$\mu'' = 4\pi M_{\text{eff}}\gamma\omega\alpha_{\text{eff}} \frac{(4\pi M_{\text{eff}} + H_{\text{K}}^{\text{dyn}})^2(1+\alpha_{\text{eff}}^2) + \omega^2}{[\omega_{\text{R}}^2(1+\alpha_{\text{eff}}^2) - \omega^2]^2 + [\alpha_{\text{eff}}\omega\gamma(4\pi M_{\text{eff}} + 2H_{\text{K}}^{\text{dyn}})]^2} \tag{3}$$

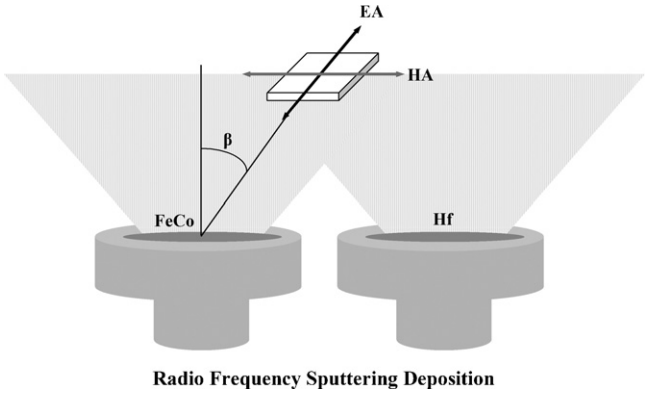

Fig. 1. Schematic sketch of the gradient sputtering deposition system.

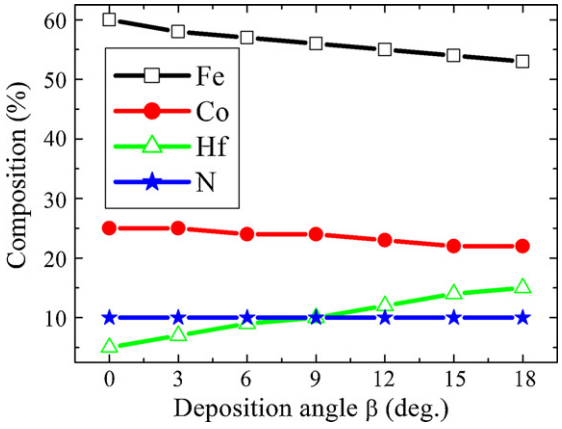

Fig. 2. Composition variation of FeCoHfN thin films with deposition angle.

Here, M_{eff}, $H_{\text{K}}^{\text{dyn}}$ and ω_{R} ($\omega_{\text{R}} = 2\pi f_{\text{FMR}}$) are the effective magnetization, dynamic magnetic anisotropy and ferromagnetic resonance frequency, respectively. Using the above equation, we can fit the permeability curves as in Fig. 3(c) and (d). The deposition angle dependences of $H_{\text{K}}^{\text{dyn}}$ and M_{eff} derived from the above curve-fitting are plotted in Fig. 4(a) together with the static anisotropy field $H_{\text{K}}^{\text{sta}}$ extracted from the slope of rotational-like magnetization curve on the hard axis [15]. For the sake of accuracy in estimating $H_{\text{K}}^{\text{sta}}$ we employed the virgin curve approximation technique [17] described as follows. First a virgin curve was approximated by averaging the forward and the backward branches of the hard axis loops [17]. Then $H_{\text{K}}^{\text{sta}}$ was extracted by extrapolating the slope of the obtained virgin curve at original point. This technique ensures that the estimated $H_{\text{K}}^{\text{sta}}$ is accurate even in the case of relatively high coercivity and remanence in hard axis loops. It is observed that both static and dynamic magnetic anisotropy fields are increased with the deposition angle β. The effective magnetization however is decreased due to the decreased of FeCo component as seen in Fig. 2 and discussed above. It is observed that there is a substantial discrepancy between static and dynamic magnetic anisotropy. With our meticulous estimation of $H_{\text{K}}^{\text{sta}}$ mentioned earlier, it is very unlikely that the discrepancy comes from the measurement error of $H_{\text{K}}^{\text{sta}}$ from hysteresis loops. The discrepancy however can be explained within the framework of Hoffmann's ripple theory [18]. According to Hoffmann, there is an additional effective isotropic field that contributes to the anisotropy field obtained from permeability spectra in addition to the static intrinsic anisotropy field. This additional effective field dependent on a so-called ripple constant may originate from the local random anisotropies which are in isotropic distribution [18–21] and as a result it is not included in $H_{\text{K}}^{\text{sta}}$ from the static measurement as that from the dynamic measurement [19,20]. The difference between $H_{\text{K}}^{\text{sta}}$ and $H_{\text{K}}^{\text{dyn}}$ may be assigned as rotatable magnetic anisotropy field (so-called dynamically induced internal field or ripple field) [22]. Similar to exchange-biased system [23,24], the rotatable anisotropy has a close relationship with the coercivity as shown in Fig. 3(b) suggesting that the physical origin of coercivity variation may presumably be the same as the arising of rotatable anisotropy. The enhancement of coercivity in this case may be because of the increase of uniaxial anisotropy with the off-center of the substrate.

In principle, the FMR frequency can be estimated by determining the peak position of the permeability spectra but this is not easy for the case of broad frequency linewidth. It is thus more accurate to derive the FMR frequency (f_{FMR}) from the fitting curves in Fig. 3. In

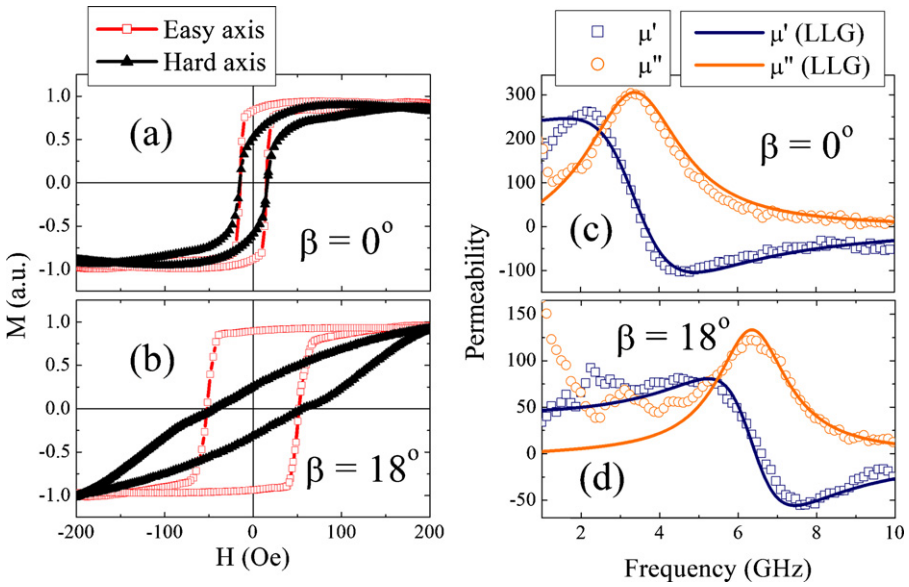

Fig. 3. Hysteresis loops and permeability spectra for FeCoHfN thin films for deposition angle $\beta = 0^\circ$ [(a) and (c)] and $\beta = 18^\circ$ [(b) and (d)].

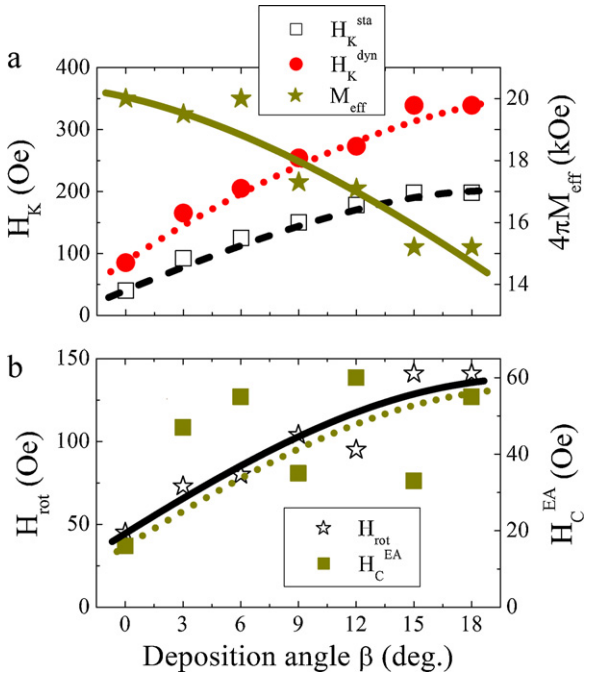

Fig. 4. (a) Variations of static (H_K^{sta}) and dynamic (H_K^{dyn}) magnetic anisotropy fields and effective magnetization ($4\pi M_{eff}$) with the deposition angle. (b) Variation of rotatable anisotropy field together with the variation of coercivity along easy axis as a function of deposition angle. Lines serve as a guide to the eyes.

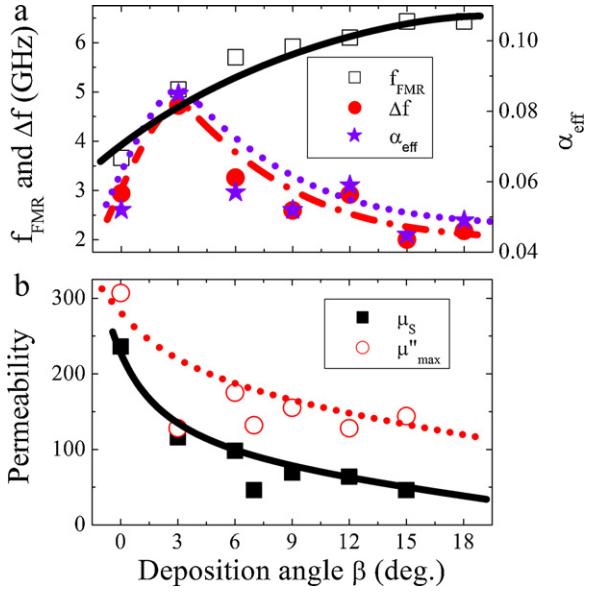

Fig. 5. (a) Deposition angle dependences of ferromagnetic resonance frequency f_{FMR}, frequency linewidth Δf and effective damping coefficient α_{eff}. (b) Deposition angle dependences static permeability (μ_s) and the maximum imaginary permeability (μ''_{max}). Lines serve as a guide to the eyes.

particular, f_{FMR} can be obtained by Kittel equation [25]:

$$f_{FMR} = \frac{\gamma}{2\pi}\sqrt{H_K^{dyn}(H_K^{dyn} + 4\pi M_{eff})} \quad (4)$$

The variations of FMR frequency (f_{FMR}), frequency linewidth (Δf) and effective damping coefficient (α_{eff}) with deposition angle are summarized in Fig. 4(a). The effective damping coefficient α_{eff} is derived from curve-fitting and the frequency linewidth Δf is determined from the following formula [20]:

$$\Delta f = \frac{\gamma\alpha_{eff}(4\pi M_{eff} + 2H_K^{dyn})}{2\pi} \quad (5)$$

The above equation explains well the similar behaviors of the frequency linewidth Δf and the effective damping coefficient α_{eff} as in Fig. 5(a). It is noticed that the effective damping coefficient is relatively high as shown in Fig. 5(a). This high damping factor may presumably come from the wide distribution of magnetic anisotropy which is evident by the observation of the relatively high remanence in hard axis loops [15]. The variation observed in the damping factor versus deposition angle in Fig. 5(a) may also be possibly interpreted in terms of the distribution of magnetic anisotropy as one can see in Fig. 3(a) and (b) that the loop of the low oblique deposition angle deposited sample show a significantly higher remanence than that of the high angle deposited one. Generally speaking, this behavior seems reasonable that as the deposition angle increases the induced magnetic anisotropy field (H_K) is increased concurrently with the more relatively uniform dis-

tribution of H_K. As a result of it the decrease of α_{eff} with deposition angle occurs as in Fig. 5(a). Still there is a peculiar unexplainable peak that requires further study in the future. One can see clearly in Fig. 5(a) that by changing deposition angle β the ferromagnetic resonance frequency can be tailored from 3.66 GHz to 6.43 GHz which is quite promising for microwave applications. Fig. 5(b) shows the variations of static permeability (μ_s) which is derived from the LLG curves at zero frequency and the maximum imaginary permeability (μ''_{max}) estimated from permeability spectra. Consistent with Acher's law [26,27], the reduction of μ_s with substrate position is due to the increase of f_{FMR} while the decrease of μ''_{max} is due to the broadening of the frequency linewidth.

4. Summary and conclusion

In short, this study is focused on the influence of deposition angle in co-sputtering system on the dynamic magnetization of FeCoHfN thin films. A discrepancy between static and dynamic magnetic anisotropy field was observed suggesting the existence of rotatable anisotropy which is interpreted by using the ripple theory. By varying deposition angle, the ferromagnetic resonance frequency of the thin films can be tailored from 3.66 GHz to 6.43 GHz implying that FeCoHfN thin films fabricated by the present method are suitable for microwave applications.

Acknowledgements

The financial support from the DSO National Laboratories and the Defence Research and Technology Office (DRTech) of Singapore is gratefully acknowledged.

References

[1] S.X. Wang, N.X. Sun, M. Yamaguchi, S. Yabukami, Nature 407 (2000) 150.
[2] K. Ikeda, K. Kobayashi, K. Ohta, R. Kondo, T. Suzuki, M. Fujimoto, IEEE Trans. Magn. 39 (2003) 3057.
[3] S. Li, Z. Huang, J-.G. Duh, M. Yamaguchi, Appl. Phys. Lett. 92 (2008) 092501.
[4] A.N. Lagarkov, S.A. Maklakov, A.V. Osipov, D.A. Petrov, K.N. Rozanov, I.A. Ryzhikov, M.V. Sedova, S.N. Starostenko, I.T. Yakubov, J. Commun. Technol. Electron. 54 (2009) 596.
[5] T.J. Klemmer, K.A. Ellis, L.H. Chen, B. van Dover, S. Jin, J. Appl. Phys. 87 (2000) 830.
[6] L.H. Chen, T.J. Klemmer, K.A. Ellis, R.B. van Dover, S. Jin, J. Appl. Phys. 87 (2000) 5858.
[7] A. Hashimoto, S. Nakagawa, M. Yamaguchi, IEEE Trans. Magn. 43 (2007)2627.
[8] S. Ge, S. Yao, M. Yamaguchi, X. Yang, H. Zuo, T. Ishii, D. Zhou, F. Li, J. Phys. D: Appl. Phys. 40 (2007) 3660.
[9] X. Wang, F. Zheng, Z. Liu, X. Liu, D. Wei, F. Wei, J. Appl. Phys. 105 (2009) 07B714.
[10] F. Xu, X. Chen, Y.G. Ma, N.N. Phuoc, X.Y. Zhang, C.K. Ong, J. Appl. Phys. 104 (2008) 083915.
[11] N.D. Ha, M.H. Phan, C.O. Kim, Nanotechnology 18 (2007) 155705.
[12] K. Seemann, H. Leiste, Ch. Klever, J. Magn. Magn. Mater. 321 (2009) 3149.
[13] C-.L. Kuo, S. Li, J-.G. Duh, Appl. Surf. Sci. 254 (2008) 7417.
[14] Y. Liu, L.F. Chen, C.Y. Tan, H.J. Liu, C.K. Ong, Rev. Sci. Instrum. 76 (2005) 063911.
[15] N.N. Phuoc, F. Xu, C.K. Ong, J. Appl. Phys. 105 (2009) 113926.
[16] T.L. Gilbert, IEEE Trans. Magn. 40 (2004) 3443.
[17] S.M. Zhou, L. Sun, P.C. Searson, C.L. Chien, Phys. Rev. B 69 (2004) 024408.
[18] H. Hoffman, IEEE Trans. Magn. 4 (1968) 32.
[19] J. Rantschler, C. Alexander Jr., J. Appl. Phys. 93 (2003) 6665.
[20] G. Suran, H. Ouahmane, I. Iglesias, M. Rivas, J. Corrales, M. Contreras, J. Appl. Phys. 76 (1994) 1749.
[21] F. Xu, X.Y. Zhang, Y.G. Ma, N.N. Phuoc, X. Chen, C.K. Ong, J. Phys. D: Appl. Phys. 42 (2009) 015002.
[22] I.S. Jeong, A.P. Valanju, R.M. Walser, J.H. Herring, J. Appl. Phys. 64 (1988) 5679.
[23] J. McCord, R. Mattheis, D. Elefant, Phys. Rev. B 70 (2004) 094420-1.
[24] B.K. Kuanr, S. Maat, S. Chandrashekariaih, V. Veerakumar, R.E. Camley, Z. Celinski, J. Appl. Phys. 103 (2008) 07C107.
[25] C. Kittel, Phys. Rev. 71 (1947) 270.
[26] O. Acher, A.L. Adenot, Phys. Rev. B 62 (2000) 11324.
[27] O. Acher, S. Dubourg, Phys. Rev. B 77 (2008) 104440.